

## Endoscopic Observation of Tissue by Narrowband Illumination

Kazuhiro GONO<sup>1,2</sup>, Kenji YAMAZAKI<sup>1</sup>, Nobuyuki DOGUCHI<sup>1</sup>, Tetsuo NONAMI<sup>1</sup>,  
Takashi OBI<sup>2</sup>, Masahiro YAMAGUCHI<sup>2</sup>, Nagaaki OHYAMA<sup>3</sup>, Hirohisa MACHIDA<sup>4</sup>,  
Yasushi SANŌ<sup>4</sup>, Shigeaki YOSHIDA<sup>4</sup>, Yasuo HAMAMOTO<sup>5</sup> and Takao ENDO<sup>5</sup>

<sup>1</sup>Olympus Optical Co., Ltd., Ishikawa-cho, Hachioji-shi, Tokyo 192-8507, Japan

<sup>2</sup>Imaging Sciences and Engineering Laboratory, Tokyo Institute of Technology,  
4259 Nagatsuda-cho, Midoriku, Yokohama-shi, Kanagawa 226-8503, Japan

<sup>3</sup>Frontier Collaborative Research Center, Tokyo Institute of Technology, Kanagawa 226-8503, Japan

<sup>4</sup>Dep. of Gastroenterology and Endoscopy, National Cancer Center Hospital East,  
6-5-1 Kashiwanoha, Kashiwa-shi, Chiba 277-8577, Japan

<sup>5</sup>First Department of Internal Medicine, Sapporo Medical University, S-1, W-16, Chuo-ku, Sapporo 060-8543, Japan

(Received February 20, 2003; Accepted May 14, 2003)

We propose a new illumination method for a medical endoscope: narrow band imaging (NBI), in which the spectral bandwidth of the filtered light is narrowed. To confirm how the spectral specifications of the filtered light influence a reproduced image, an experiment was conducted observing the endoscopic images of the back mucosa of a human tongue. In addition, the effect of NBI on endoscopic images was investigated through preliminary clinical tests in colonoscopy and upper gastrointestinal endoscopy. It has been shown that NBI can enhance the capillary pattern and the crypt pattern on the mucosa. These patterns are useful features for diagnosing an early cancer.

**Key words:** video endoscope, tissue imaging, blood vessel, narrowband illumination, clinical test

### 1. Introduction

Recently the importance of endoscopy has been attracting a great deal of interest from the viewpoint of the early therapy of a tumor. Several attempts have been conducted on the progressive development of the video endoscope system to improve the accuracy of an endoscopic diagnosis. In addition to improvements of the CCD resolution of an endoscope, the luminance of the illumination source or the color reproduction of the whole system, a magnified endoscope<sup>1)</sup> and chromoscopy,<sup>2,3)</sup> have also been proposed. Several special endoscopes have been studied, which use an invisible light such as fluorescence<sup>4)</sup> and infrared.<sup>5)</sup> These instruments are expected to detect a small polyp on the mucosa and the tumor under the mucosa.

It is well known that estimating the pathology of a colon polyp is possible by observing the crypt orifice (so-called pit-pattern) of colonic glands using a magnifying endoscope.<sup>6–8)</sup> Several groups have reported that the capillary pattern on the mucosa is also an important feature for the early diagnosis of a gastrointestinal disease.<sup>9,10)</sup> It is therefore necessary to see such a pattern in more detail for diagnosing early cancer.

We have attempted a novel technique, narrow band imaging (NBI), to enhance certain histological features such as the capillary and the pit patterns in endoscopic images. The NBI is a simple technology that uses optical filters for RGB sequential illumination and narrows its bandwidth of the spectral transmittance. The aim of the present paper is to show how spectral specifications of the optical filter influence the reproduced image and to confirm the clinical efficiency of the NBI. We conducted a newly experiment observing the endoscopic images of the back mucosa of a human tongue. From the results, we confirmed that NBI has an advantage over the conventional system in observing the capillary pattern. Three narrowband filters were assigned to the RGB color channel, and preliminary clinical tests of the

NBI were carried out. We were able to obtain an enhanced color image in which the histological features were seen easily.

### 2. Method

Sanbongi *et al.*<sup>11)</sup> reported on the reflectance spectra of the gastrointestinal mucosa using an endoscopic spectroscopy system. From their results, it is obvious that the absorbance bands of the hemoglobin exist within the spectrum of colon mucosa. This indicates that the hemoglobin acts as a main absorber in the gastrointestinal mucosa. To understand the reflectance spectrum of any tissue, the scattering process as well as the absorption should be considered. The tissue has various structures, and these complicated structures probably act as scattering elements. There have been several investigations to understand the mechanisms of the scattering from tissue structures.<sup>12,13)</sup> Zonios *et al.* estimated that the mean diameter of scattering particles in the human colon is about 0.56  $\mu\text{m}$  by Mie scattering theory.<sup>14)</sup> They also demonstrated that the scattering coefficient of the colon tissue monotonically decreases as the wavelength increases. It is likely that the wavelength dependence of the light's penetration depth is due to the absorption and the scattering. Marchesini *et al.* also reported the optical coefficients of colon tissues.<sup>15)</sup> We show that the light's penetration depth depends on the wavelength by the Monte Carlo simulation. We used the Monte Carlo code (MCML) proposed by Wang *et al.*<sup>16)</sup> The reduced scattering coefficients and the absorption coefficients are taken from Marchesini (Fig. 2 in Marchesini *et al.*). The other conditions of the simulation are the following:

- Tissue model : 1mm thickness slab in the air
- Scattering anisotropy ( $g$ ) : 0.9 (typical value of biological tissue)
- Refractive index : 1.3(tissue), air(1.0)
- Incident photon : 10,000,000 photons

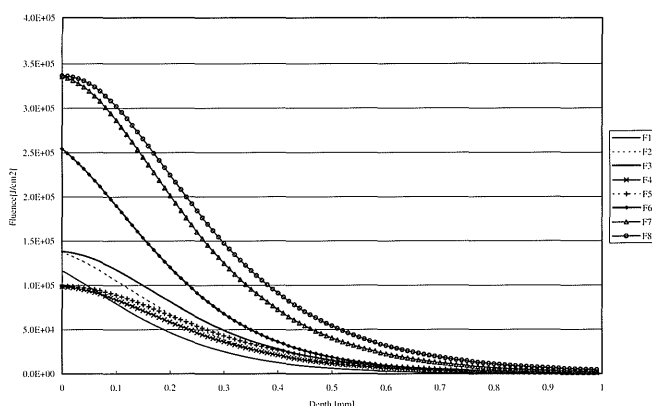


Fig. 1. Fluence at photon incident point against  $z$  axis.

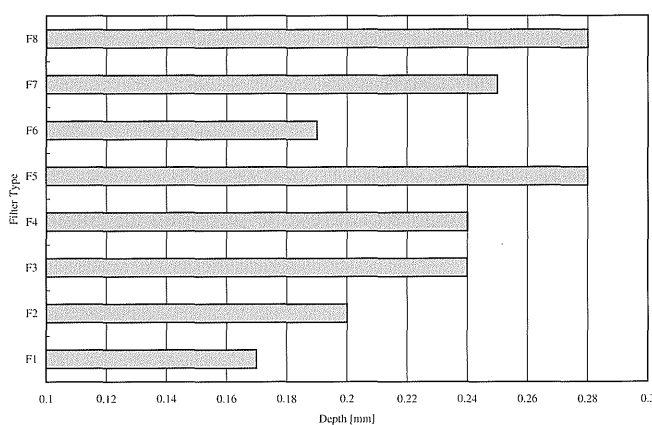


Fig. 2. Penetration depth of each filtered light.

- Wavelength : 400–700 nm, 5 nm step

Figure 1 shows the photon fluence along  $z$ -axis at the photon incident point. The fluence decreases with an increase in depth. In our study, it is assumed that the penetration depth is the depth with a half fluence value. Figure 2 shows the penetration depth in each filtered light (the spectral specifications of the filter are shown in Table 1). The results in Fig. 2 demonstrate the following:

- The center wavelength and the bandwidth have an effect on the penetration depth.
- The difference in penetration depth between the narrowband filters (from F1 to F5) is larger than that between the broadband filters (from F6 to F8).

Additionally, we can consider imaging of the blood vessels as follows.

- Light in long wavelength (ex. 600 nm) is outside of the hemoglobin absorption band (ex. 420 nm, 550 nm). Therefore, in order to have a large contrast between the blood vessels and the adjacent mucosa, the blood vessels must be very thick.
- Light in short wavelength (ex. 420 nm, 550 nm) is within the hemoglobin absorption band. Therefore, the thin blood vessels have an enough contrast to see it clearly.
- Gastrointestinal mucosa has a layered structure and the pathological features in each layer are very different

Table 1. Spectral specifications (center wavelength and FWHM) of filters.

	F1	F2	F3	F4	F5	F6	F7	F8
Center	415 nm	445 nm	500 nm	540 nm	600 nm	420 nm	540 nm	610 nm
FWHM	30 nm	30 nm	30 nm	20 nm	20 nm	100 nm	80 nm	80 nm

from each other. The mucous membrane, the top layer, has many capillaries, the sub-mucosa has some thick blood vessels.

From the above considerations, we expect that the optical enhanced imaging is possible using a narrowband filter set, which has a great variation in penetration depth.

To confirm the feasibility of NBI, comparative experiments were conducted between it and a conventional illumination unit.

The medical video endoscope system (EVIS 240, OLYMPUS OPTICAL Co., Ltd.), which is equipped with sequential illumination, was used in our experiments. The filter wheel in the illumination unit has three optical filters. In the conventional unit, three broadband type filters (refer to F6 to F8 in Table 1) are used. The spectra of these filters divide the visible wavelength range into three bands. In the NBI, three narrowband filters (F1 to F5 in Table 1) are used instead of the broadband filters. Three filtered lights sequentially illuminate the tissue as the filter wheel rotates. The reflected light from the tissue is converted to image signals with a monochromatic CCD at the distal end of the video endoscope. The monochromatic image signal corresponding to each filtered illumination is formed by synchronizing the sequential illumination process and the conversion process by the CCD. To display a color image on the CRT, each monochromatic image signal is assigned to the B/G/R color channel. The frame grabber (METOR II/MC4; Matrox Electronic Systems, Ltd.), which can convert the NTSC-RGB component analog signal to a digital one with 8 bits in each color channel, was used to record the image. A magnified endoscope (GIF-Q240Z, OLYMPUS OPTICAL Co., Ltd.), which has the 80-fold optically magnification capability, was employed in our study.

The feasibility of NBI was confirmed by considering the following three issues:

- (1) Influence of the spectral specification of the optical filter on the contrast of blood vessels in the image.
- (2) The optimal filter set for color imaging.
- (3) The clinical benefit of using NBI in endoscopy.

For issue (1), an experiment with the back mucosa of a human tongue was carried out using five narrowband filters and three broadband filters. The blood vessel structure of the human tongue is similar to that of gastrointestinal mucosa.<sup>17,18)</sup> The spectral specifications of these filters are shown in Table 1. The spectral shape of each filter is an almost Gaussian. The spectral specifications of the broadband filters (F6, F7, F8) are similar to the filters used in a conventional illumination unit. Images of the back mucosa of the tongue were captured by eight filters, and the vascular patterns in the images were compared and subjectively evaluated.

For issue (2), in the experiment with the back mucosa of a human tongue three types of filter set were used. Assign-

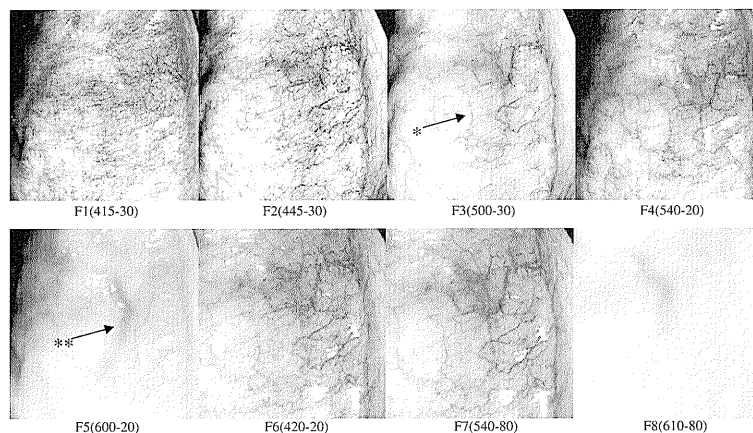


Fig. 3. NBI images of back membrane of a human tongue.

Table 2. Filter sets and assignments of band image to color channel for color imaging. The values in parentheses represent center wavelength - FWHM.

	B channel	G channel	R channel
Set A	F1(415-30)	F4(540-20)	F5(600-20)
Set B	F1(415-30)	F2(445-30)	F3(500-30)
Set C	F6(420-100)	F7(540-80)	F8(610-80)

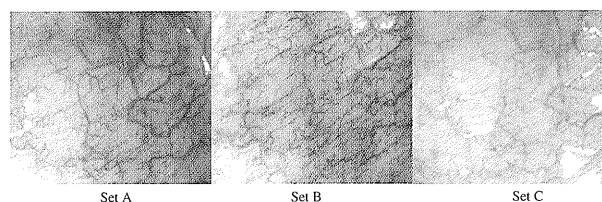


Fig. 4. NBI color images of back membrane of a human tongue with different filter combinations.

ments of the filter set to color channel are shown in Table 2, we assigned BGR color channels in order of wavelength. The appearance of the human tongue blood vessels in the narrowband images was subjectively evaluated.

For issue (3), preliminary clinical tests of NBI were conducted in a colonoscopy of a small polyp and in an upper gastrointestinal endoscopy of Barrett's esophagus. Comparative evaluation between the conventional illumination and the NBI examined the same tissue portion in both cases. The filter set used in the NBI examination process was set B (see Table 2).

### 3. Results and Discussion

Figure 3 shows the images of the back mucosa of the tongue. From narrow-band images (from F1 to F5), it is found that the appearance of blood vessels depends on the center wavelength and thickness of the blood vessels. Thick blood vessels, which are marked by double asterisks on 605 nm (F5), cannot be seen well in the 540 nm (F4) image, and cannot be found at all on the 415 nm (F1). The loop pattern of the blood vessel, which is marked by an asterisk, also cannot be seen on 415 nm (F1). However, the capillaries on the mucosa surface can be seen most clearly on 415 nm (F1). In the case of the broadband filter, the blood vessel pattern of F6 is similar to that of F7. However, in the narrowband filter, quite different images were obtained using F1 and F4. These results indicate that the human tongue has a blood vessel structure which varies depending on depth, and the narrowband illumination can obtain an image reflecting the vessels at their actual depth. The capillary patterns can be seen vividly in F1 but not in other images. Kienle *et al.* studied how the wavelength of the illumination

depends on the reproduced color of a vein under the skin using a thin glass tube phantom enclosing whole blood, in a lipid colloid.<sup>19)</sup> It was also shown that the contrast of the vein phantom depends on its depth, its thickness and the scattering property of its ambient medium. Our experimental results corroborate to their conclusions.

Figure 4 shows the NBI colored images of the back membrane of a human tongue, in set C the color looks more natural than in set A or set B. Lower contrast of the blood vessel patterns makes it difficult to see the fine capillary patterns, which are easily seen in set A and set B. In Fig. 4 (set A) the capillaries in the 415 nm image appear in a yellowish pattern. The blood vessels in the 540 nm image are seen in a magenta pattern and the thick blood vessels in the 605 nm image in a cyan pattern. These color differences reflect the differences in depth distribution of the blood vessels. This will be an advantageous if information about the tissue structure can be estimated from a colored image. However, the capillary pattern on the mucosa is difficult to examine because of its yellowish color. In set B of the figure this pattern is shown in brown because we assigned F1 to B channel and F2 to G channel. The brown pattern is seen more clearly than in set A. From the results, it is found that a center wavelength of narrowed bandwidth filters should be selected depending on the aim of color reproduction. In this study, we especially focused on the enhancement of the capillary and the pit pattern because these patterns are important to the diagnosis of a tumor in its early stage. Therefore, set B was used in clinical tests.

Figures 5(a) and 5(b) show the endoscopic images of a small colon polyp. Figure 5(a) is an image taken with the

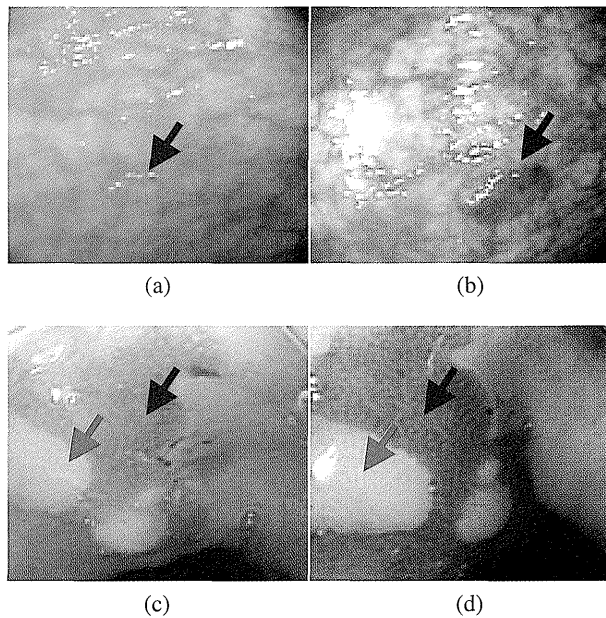


Fig. 5. Colon polyp (upper series) and Barrett's esophagus (lower series).

conventional illumination unit and Fig. 5(b) is taken with the NBI. In Fig. 5(b), the polyp is shown in brown because of the increased capillaries, which are reproduced in F1 (B channel) and F2 (G channel), on the surface of the colon mucosa. From the preliminary result, NBI is expected to be a useful tool to identify a small polyp in a colonoscopy instead by chromoscopy.

Figures 5(c) and 5(d) show endoscopic images of Barrett's mucosa at the esophagus-stomach junction; (c) is the image taken with the conventional illumination unit, while (d) is that with the NBI. The boundary between the stratified squamous epithelium (green arrows) and Barrett's mucosa (blue arrows), and the pit pattern on Barrett's mucosa is seen more vividly in Fig. 5(d) than in Fig. 5(c). Since the stratified squamous epithelium has a closely packed tissue structure, the observation light, which is less than 500 nm long, hardly penetrates this type of tissue. Most of the lights are scattered and reflected from the stratified squamous epithelium. However, the light in longer wavelengths such as 605 nm, which is used in the conventional illumination unit, can easily penetrate the stratified squamous epithelium, and therefore this is shown as white color regions in the NBI. The pit pattern on Barrett's mucosa has many capillaries around the crypt. In the NBI, this pit pattern is seen with a brown texture, similar to the case of the colon polyp. Endo *et al.* reported that the pit pattern of Barrett's mucosa is useful in classifying to the high-risk portion of Barrett's cancer.<sup>20)</sup> Therefore, NBI is expected to be a useful tool for detecting this high-risk portion based on diagnosis of the pit pattern.

Figures 6(a) and 6(b) show magnified endoscopic images of a colon polyp (early cancer in the rectum); (a) is an image taken with the conventional illumination unit, and (b) is that with the NBI. In the NBI, the texture of this pit pattern can be seen clearly. Figures 7(a) and 7(b) show the pathology as hemotoxilyn-eosin stain images of the same colon polyp as illustrated in Figs. 6(a) and 6(b); (b) is a highly magnified

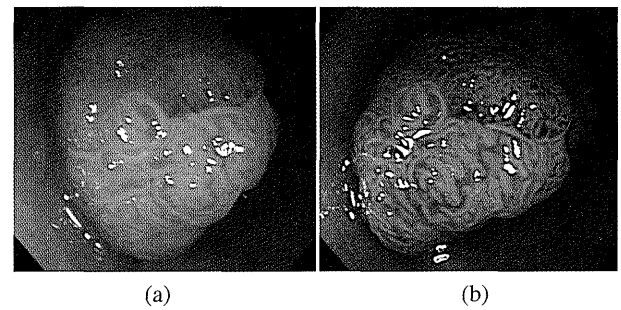


Fig. 6. Colon polyp (lower rectum, Isp type early cancer, 8 mm diameter).

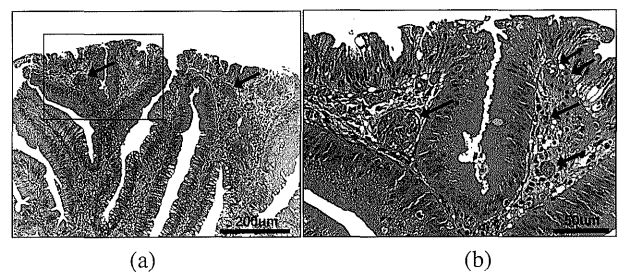


Fig. 7. Histological findings of the rectal polyp illustrated in Fig. 6. Capillary vessels filled with red blood cells are located on the surface of this polyp (arrow).

image of part of (a) (the square area). Capillary vessels filled with red blood cells are located at the surface of this polyp (arrow). There are many capillary vessels around the colonic gland; in Fig. 6(a) and Fig. 6(b), the colonic gland has a tubular shape of which the diameter is about 50–100  $\mu\text{m}$ . The brown pattern on the polyp [Fig. 6(b)] around the whitish pattern is believed to be capillary vessels around the colonic gland. These capillary vessels were clearly captured on the F1 and F2 band images. Considering that most of these vessels are on near the surface (about 150  $\mu\text{m}$  from the surface), we can estimate the penetration depth of the F1 and F2 filtered light as about 150  $\mu\text{m}$ . Our estimate agrees with the result of the Monte Carlo simulations in Fig. 2.

#### 4. Conclusion

We have proposed a new endoscopic imaging: the NBI. The NBI system can be installed simply by changing the optical filters for sequential illumination from the conventional broadband type to the narrowband type. In preliminary clinical tests, we confirmed that NBI has an advantage over the conventional system. It is able to represent more clearly the important features, i.e. capillary patterns and the boundary between different types of tissue, which are necessary for diagnosing a tumor in its early stage. We plan to report quantitative evaluations of the blood vessels' contrast in narrowband image and the optimal filter set for color imaging in another paper.

#### Acknowledgments

The work was supported in part by a Grant for Scientific Research Expenses for Health and Welfare Programs and the Foundation for the

Promotion of Cancer Research and by 2nd-Term Comprehensive 10-year Strategy for Cancer Control. The authors gratefully acknowledge useful and stimulating discussions about tissue optics with H.Haneishi and N.Tsumura at Chiba University.

#### References

- 1) K. Tobita: *Dig. Endosc.* **13** (2001) 121.
- 2) M. B. Fennerty: *Can. J. Gastroenterol.* **13** (1999) 423.
- 3) M. Irene Canto: *Gastrointest. Endosc.* **49** (1999)12.
- 4) S. Takehana, M. Kaneko and H. Mizuno: *Diag. Therap. Endo.* **5** (1999) 59.
- 5) K. Iseki, M. Tatsuta, H. Iishi, N. Sakai, H. Yano and S. Ishiguro: *Gastrointest. Endosc.* **52** (2000) 755.
- 6) S. Kudo, S. Hirota, T. Nakajima, S. Hosobe, H. Kusaka, T. Kobayashi, M. Himori and A. Yagyu: *J. Clin. Pathol.* **47** (1994) 880.
- 7) S. Kudo, S. Tamura, T. Nakajima, H. Yamano, H. Kusaka and H. Watanabe: *Gastrointest. Endosc.* **44** (1996) 8.
- 8) S. Kudo, H. Kashiba, T. Nakajima, S. Tamura and K. Nakajo: *World J. Surg.* **21** (1997) 694.
- 9) Y. Kumagai, H. Inoue, K. Nagai, T. Kawano and T. Iwai: *Endosc.* **34** (2002) 369.
- 10) K. Yagi, A. Nakamura and A. Sekine: *Endosc.* **34** (2002) 376.
- 11) M. Sambongi, M. Igarashi, T. Obi, M. Yamaguchi, N. Ohyama, M. Kobayashi, Y. Sano, S. Yoshida and K. Gono: *Med. Phys.* **27** (2000) 1396.
- 12) J. R. Mourant, J. P. Freyer, A. H. Hjielscher, A. A. Eick, D. Shen and T. M. Johnson: *Appl. Opt.* **37** (1998) 3586.
- 13) J. R. Mourant, M. Canpolat, C. Brocker, O. Esponda-Ramos, T. M. Johnson, A. Matanock, K. Stetter and J. P. Freyer: *J. Biomed. Opt.* **5** (2000) 131.
- 14) G. Zonios, L. T. Perelman, V. Backman, R. Manoharan, M. Fitzmaurice, J. Van Dam and M. S. Feld: *Appl. Opt.* **38** (1999) 6628.
- 15) R. Marchesini, E. Pignoli, S. Tomatis, S. Fumagalli, A. E. Sichirollo, S. D. Palma, M. D. Fante, P. Spinelli, A. C. Croce and G. Bottirol: *Laser. Surg. Med.* **15** (1994) 351.
- 16) L-H, Wang, S. L. Jacques and L-Q, Zheng: *Comput. Methods Programs Biomed.* **47** (1995) 131.
- 17) M. A. Konerding, E. Fait and A. Gaumann: *Br. J. Cancer* **84** (2001) 1354.
- 18) A. Amar, A. F. Giovanini, M. P. Rosa, H. O. Yamassaki, M. B. Carvalho and A. Rapoport: *Rev. Assoc. Med. Bras.* **48** (2002) 204.
- 19) A. Kienle, L. Lilge, A. Vitkin, M. S. Patterson, B. C. Wilson, R. Hibst and R. Steiner, *Appl. Opt.* **35** (1996) 1151.
- 20) T. Endo, T. Awakawa, H. Takahashi, Y. Arimura, F. Itoh, K. Yamashita, S. Sasaki, H. Yamamoto, X. Tang and K. Imai: *Gastroint. Endosc.* **55** (2002) 641.